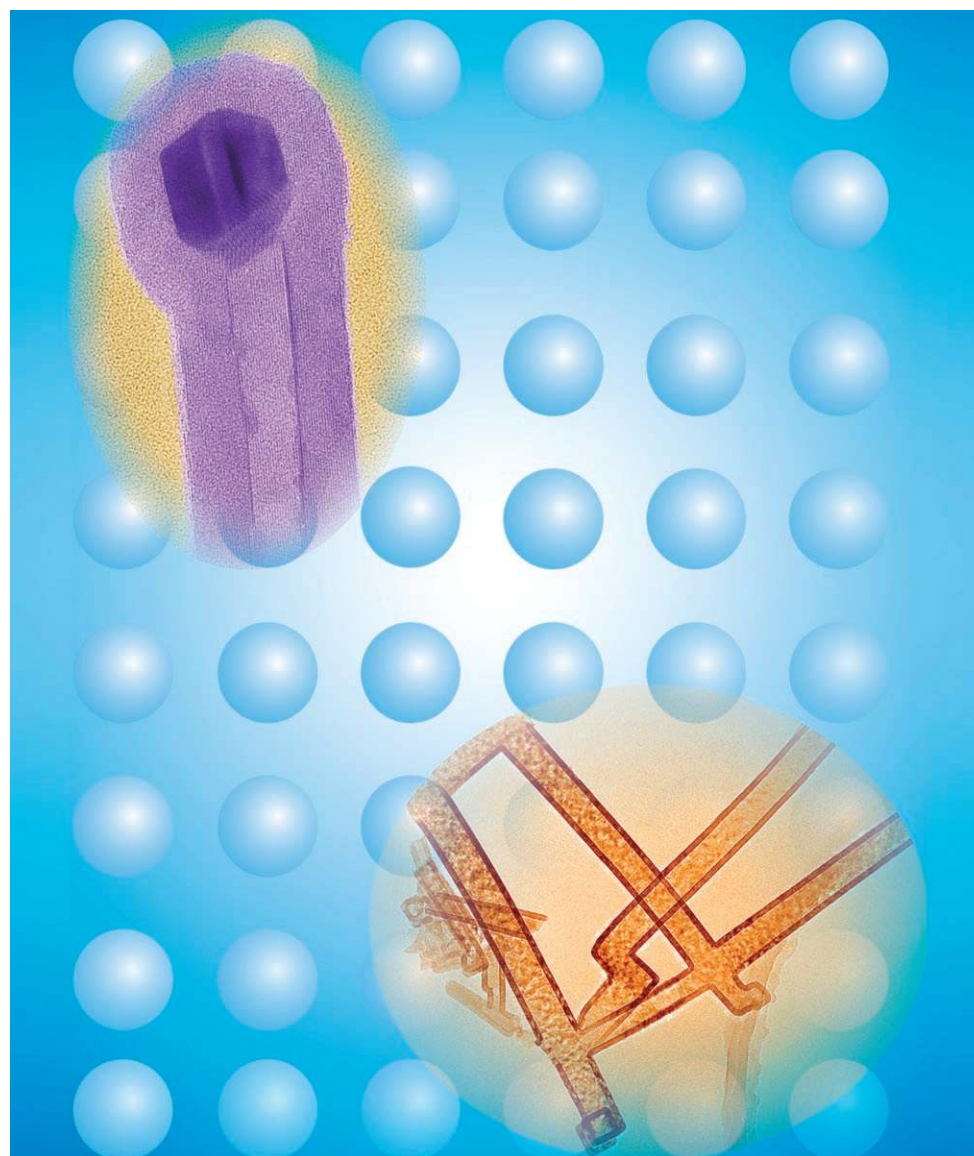


DOI: 10.1002/sml.200700382

Formation of Nanotubes and Hollow Nanoparticles Based on Kirkendall and Diffusion Processes: A Review

Hong Jin Fan, Ulrich Gösele, and Margit Zacharias*

Novel nano-objects are fabricated using the Kirkendall effect.

NANO MICRO
small

From the Contents

1. Introduction.....1661
2. Theoretical Considerations.....1663
3. Hollow Nanoparticles1665
4. Nanotubes.....1667
5. Conclusions and Outlook.....1670

Keywords:

- diffusion
- hollow nanoparticles
- Kirkendall effect
- nanotubes
- solid-state reactions

The Kirkendall effect is a consequence of the different diffusivities of atoms in a diffusion couple causing a supersaturation of lattice vacancies. This supersaturation may lead to a condensation of extra vacancies in the form of so-called "Kirkendall voids" close to the interface. On the macroscopic and micrometer scale these Kirkendall voids are generally considered as a nuisance because they deteriorate the properties of the interface. In contrast, in the nanoworld the Kirkendall effect has been positively used as a new fabrication route to designed hollow nano-objects. In this Review we summarize and discuss the demonstrated examples of hollow nanoparticles and nanotubes induced by the Kirkendall effect. Merits of this route are compared with other general methods for nanotube fabrication. Theories of the kinetics and thermodynamics are also reviewed and evaluated in terms of their relevance to experiments. Moreover, nanotube fabrication by solid-state reactions and non-Kirkendall type diffusion processes are covered.

1. Introduction

Hollow nano-objects can consist of either organic or inorganic materials: The former refers mainly to carbon nanotubes or other hollow carbon nanoparticles (e.g., C_{60}), whereas the latter could be any type of material according to recent literature. The shell structure can be fullerene-like (i.e., single- or multilayered), for which graphite, WS_2 , and BN are the paradigm materials, but is single-crystalline or poly-crystalline (i.e., nonlayered) in most cases. Starting with C_{60} in 1985 by Smalley and co-workers,^[1] carbon nanotubes in 1991 by Iijima,^[2] and the subsequent discovery of fullerene-like WS_2 nanotubes and nanoparticles (NP) by Tenne et al.,^[3] hollow NP fabrication has been extended to a wide spectrum of materials ranging from single elements to ternary compounds, and from metals to semiconductors. Notable results come from the Bando–Golberg group in Tsukuba.^[4] The underlying mechanisms can be classified into two categories: first, self-organization such as self-rolling, Ostwald ripening, oriented attachment, and, recently, the Kirkendall effect; second, using sacrificial templates such as a porous matrix, solid nanowires, or NPs. A number of valuable reviews on inorganic hollow nano-objects are already available.^[5–8]

The Kirkendall effect is a classical phenomenon in metallurgy.^[9–11] It basically refers to a nonreciprocal mutual diffusion process through an interface of two metals so that vacancy diffusion occurs to compensate for the inequality of the material flow (Figure 1a and b) and that the initial interface moves. The first experiment was performed by Kirkendall in 1942 and the result was confirmed in a repeated experiment in 1947.^[9] The diffusion couple used consisted of copper and brass, which were welded together and subjected to elevated temperatures. A movement of the initial interface was observed, as a direct consequence of a faster diffusion of zinc into the copper than that of copper into the brass (the intrinsic diffusivity of Zn is ≈ 2.5 times that of Cu at 785 °C). The Kirkendall experiment established that diffu-

sion of substitutional lattice atoms involves defects that facilitate atomic jumps. In most metals and metallic alloys, as well as most other materials, these atomic defects are empty lattice sites, termed vacancies. Condensation of excess vacancies can give rise to void formation near the original interface and within the fast-diffusion side.^[12–14] Figure 1c gives an example of the Kirkendall voids at the SnPb solder–Cu interface after aging the original sample at 150 °C for 3 days.^[14] Only in a few technologically important materials such as silicon, the diffusion of lattice atoms may also be accompanied by extra lattice atoms, so-called self-interstitials.^[15,16] In these cases an imbalance of interdiffusing atoms would not lead to voids but rather to a condensation of supersaturated self-interstitials,^[17] for example, in the form of interstitial-type dislocation loops. This case will not be considered further in this article.

Formation of the Kirkendall voids deteriorates the bonding strength of the bond–pad interface or may cause wire bond failure in integrated circuits.^[18,19] Engineers try to avoid this effect by introducing diffusion barrier layers, such as, for instance, Ta as a diffusion barrier between Cu and bronze in the multifilamentary superconducting compo-

[*] Dr. H. J. Fan
Department of Earth Sciences
University of Cambridge
CB2 3EQ Cambridge (UK)
Fax: (+44) 122-333-3450
E-mail: hfano5@esc.cam.ac.uk
Prof. U. Gösele
Max-Planck-Institute of Microstructure Physics
Weinberg 2, 06120 Halle (Germany)
Prof. M. Zacharias
Faculty of Applied Science
Albert-Ludwigs-University Freiburg
Georges-Köhler-Allee, 79110 Freiburg (Germany)



Margit Zacharias has been Professor of Nanotechnology at the Faculty of Applied Science (IMTEK) of the Albert Ludwigs University Freiburg, Germany, since May 2007. Prior to joining the University of Freiburg she was Professor of Nanoelectronics and Nano-optics at the University of Paderborn after working at the Research Center Rossendorf (Leibniz Institute) and the Max Planck Institute of Microstructure Physics, Halle. She held a nontenured C3 position at the MPI Halle and was the group leader of the Nano-

wires and Nanophotonics group at the Experimental Department II from 2000–2005. Since June 2004, she coordinates the priority program on nanowires and nanotubes (SPP 1165). Her research interests include silicon-based electronics and photonics, quantum dots, science and technology of nanostructures in general, self-organized growth of nanocrystals and nanowires, and their detailed investigation and understanding.



Ulrich Gösele is Director of the Max Planck Institute of Microstructure Physics and Adjunct Professor of Electronic Materials at the Martin Luther University in Halle, Germany, as well as Adjunct Professor of Materials Science at Duke University in Durham, North Carolina. Prior to joining MPI he was Professor of Materials Science at Duke University after working in the research labs of Siemens Corporation in Munich and the MPI of Metal Research in Stuttgart, Germany. He held visiting appointments at the Atomic

Energy Board in Pretoria, South Africa, at the IBM Watson Research Center in Yorktown Heights, New York, at MIT, at NTT LSI Laboratories in Atsugi, Japan, and at Harvard University. He is a Fellow of the American Physical Society, a Fellow of the Institute of Physics (UK), a member of Leopoldina Academy, the oldest German scientific academy, and Honorary Professor of the Institute of Semiconductors of the Chinese Academy of Sciences in Beijing. His research interests include defects and diffusion processes in silicon and other semiconductors, science and technology of semiconductor wafer bonding, silicon-based photonic crystals and silicon photonics in general, self-organised fabrication of nanostructures, semiconductor nanowires, quantum dots, complex oxide nanostructures, and nanoporous films such as porous alumina.



Hongjin Fan received his Bachelor degree in physics from Jilin University (China) and his PhD from the National University of Singapore. Since 2003 he has been conducting postdoctoral research in the group of Prof. Ulrich Gösele of MPI of Microstructure Physics (Germany). He is currently a research fellow at the University of Cambridge working on wet chemistry of ferroelectric tubular structures. His research interests include semiconductor nanowires and nanotubes, compound oxide nanostructures, and atomic-layer deposition.

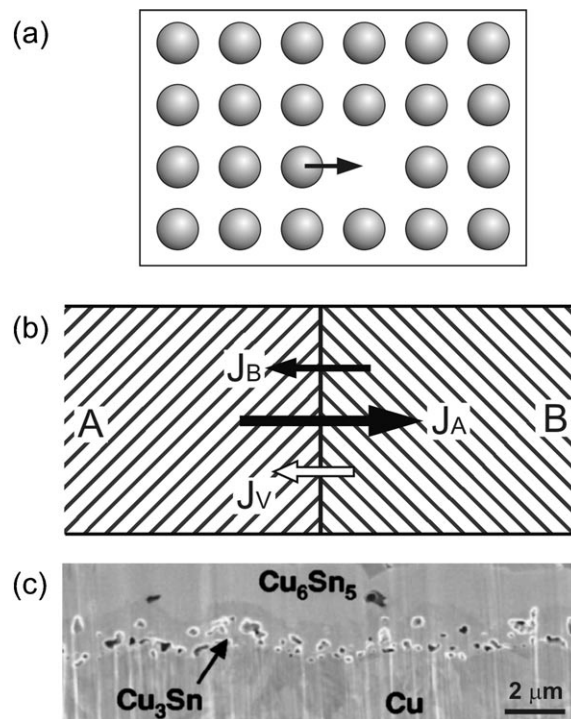


Figure 1. Schematic images of a) the vacancy mechanism of atomic diffusions and b) a nonequilibrium lattice diffusion at the interface. The consequent vacancy flux can generate a vacancy supersaturation, leading to voids in the fast-diffusion zone. c) Cross-sectional scanning electron microscopy (SEM) image of the Kirkendall voids found at the SnPb solder/Cu pad interface after aging the original sample at 150 °C for 3 days. Reproduced with permission from Ref. [14].

site.^[20] On the other hand, chemists applied this destructive effect constructively for synthesizing hollow nanostructures in a way that the Kirkendall voids coalesce into a single hollow core. Since the first demonstration in 2004,^[21] such an effect has become an interesting synthesis route to nanoscale hollow structures of various material systems, as summarized in Table 1. After more than sixty years, the Kirkendall effect receives scientific attention again in the positive context of purposely using it for fabricating designed hollow nanostructures.

In this review we will first assess the so-far available theoretic treatments (both thermodynamic and kinetic) to the Kirkendall-effect-induced hollowing process on the nanoscale. Next, we will give a full survey of the recent literature and discuss the demonstrated examples in two main categories: hollow nanoparticles and nanotubes. Focus of the discussion is on the key issues that determine successful application of the Kirkendall effect to the formation of hollow nanostructures. Also, we summarize general methods for nanotube fabrication and compare them to the Kirkendall-based route. Finally, inorganic nanotubes formed by other interface reactions and diffusion processes will be covered.

Table 1. Hollow nano- and micro-object fabrication induced by the Kirkendall effect.

Material	Morphology	Growth process	Ref.	Year of publication
BeNi, BeCo	microshells	thermal annealing of core/shell microparticles	[22]	1974
Au, Ag	nanocubes		[23]*	2002
Co ₃ S ₄ , CoO, CoSe	hollow nanocrystals	wet sulfidation or oxidation of Co nanocrystals	[21]	2004
Co ₃ S ₄ , CoSe ₂ , CoTe	hollow nanochains	solution reaction of Co nanonecklace	[24]	2006
ZnO	microcages	dry oxidation of Zn polyhedra	[25]*	2004
ZnO	dandelion	hydrothermal reaction	[26]	2004
Cu ₂ O	hollow NPs	low-temperature dry oxidation	[27]	2007
ZnS	hollow nanospheres	wet sulfidation of ZnO nanospheres	[28]	2005
PbS	hollow nanocrystals	reaction of Pb NPs with vapor S	[29]	2005
CuS	octahedral cages	sulfidation of Cu ₂ O octahedral	[30]	2006
Cu ₇ S ₄	polyhedron nanocages	sulfidation of Cu ₂ O nanocube	[31]	2005
Fe _x O _y	porous thin film	hydrothermal reaction	[32]	2005
Fe _x O _y	hollow NPs	room-temperature oxidation of < 8-nm particles	[33]	2005
ZnO	hollow NPs	low-temperature oxidation of < 20-nm particles	[34]	2007
Al _x O _y	amorphous hollow NPs	low-temperature oxidation of < 8-nm Al particles	[27]	2007
AuPt	hollow NPs	solution reaction	[35]	2004
MoS ₂	cubic microcages	solution reaction	[36]	2006
MoO ₂	hollow microcages	hydrothermal reaction	[37]	2006
Ni ₂ P, Co ₂ P	hollow NPs	wet phosphidation of Ni NPs	[38]	2007
FePt@CoS ₂	yolk-shell NPs	wet sulfidation of FePt@Co NPs	[39]	2007
Pt-Cu	core-shell NPs	solution reaction	[40]	2005
AlN	hollow nanospheres	reaction of Al NPs with NH ₃ CH ₄ gas	[41]	2006
AlN	hollow nanospheres	annealing of Al NPs in ammonia	[42]	2007
SiO ₂	hollow nanospheres	water oxidation of Si NPs	[43]	2004
Co ₃ O ₄	porous nanowires	oxidation of Co(OH) ₂ nanowires	[44]	2006
SrTiO ₃ , BaTiO ₃	porous spheres	hydrothermal reaction of TiO ₂ spheres	[45]	2006
CdS	polycrystal nanoshell	reaction of Cd nanowire with H ₂ S	[46]	2005
ZnAl ₂ O ₄	crystalline nanotubes	solid-state reaction of core/shell nanowires	[47]	2006
Ag ₂ Se	nanotubes	photodissociation of adsorbed CSe ₂ on Ag nanowires	[48, 49]	2006
Zn ₂ SiO ₄	monocrystal nanotubes	solid-state reaction of core/shell nanowires	[50]*	2007
Co ₃ S ₄	quasi monocrystal nanotubes	reaction of Co(CO ₃) _{0.35} Cl _{0.20} (OH) _{1.10} nanowires in solution with H ₂ S	[51]	2007
CuO	polycrystal nanotubes	dry oxidation of Cu nanowires	[52]	2005
CuS	monocrystal nanotubes	reaction of CuCl nanorod with H ₂ S	[53]	2007

[a] The Kirkendall effect was not pointed out by the authors but was most likely one of the growth mechanisms.

2. Theoretical Considerations

Compared to the large number of experimental demonstrations since 2004 (see Table 1), there is relatively little theoretical work on nanoscale Kirkendall diffusion effects. This is partly caused by the complexity of the reaction system itself compared to bulk planar interfaces; factors include a shortened diffusion length, interface stress, non-constant interface contact, inhomogeneous coating, and so on. These factors are trivial in macroscopic films but could make the diffusion on the nanometer scale non-Fickian.

Yin et al.^[54] dealt with the kinetics of the flux and derived the criteria and timescales for the formation of hollow nanospheres. This treatment was based on an idealized

model (Figure 2a) and a simple steady-state diffusion (i.e., a concentration profile of the vacancies within the product shell is constant with time), which is governed by Fick's first law. This means that the diffusion of mass, as well as the vacancies, is induced by the difference in atom concentration. Letting core A and shell B react to produce A_mB_n, and with $r_{in}(t)$ and $r_{out}(t)$ denoting the position of the inner and outer boundaries, respectively, of the growing shell at time t , the outward growth rate of the product layer is

$$\frac{dr_{out}}{dt} = \frac{n_A D_A \Delta C_A r_{in}(t)}{r_{out}(t)[r_{out}(t) - r_{in}(t)]} \quad (1)$$

where D_A , ΔC_A , and n_A denote the diffusivity, concentration difference, and volume density of A in the product layer, respectively. The prerequisite for formation of hollow structures is derived to be

$$\frac{n \cdot D_A |\Delta C_A|}{m \cdot D_B |\Delta C_B|} + 1 > r_{out}(t)^3 - r_{in}(t)^3 \quad (2)$$

Applying a similar treatment but in cylindrical coordinates, Prasad and Paul^[55] derived the growth rate of the product layer as well as the rate of consumption of core and shell material. Following their formulation, it is

possible to determine the radius of the core and shell, and time required to produce a single-phase nanotube. Of interest in their discussion are two qualitative scenarios for the formation of good nanotubes: the first is that the product phase should be free of dislocations and grain boundaries since these defects absorb vacancies and thus give no visible pores. However, experimentally, nanotubes that were induced by the Kirkendall effect but with tube walls composed of multigrains (effectively polycrystalline) have been shown in several publications. The other scenario states that a binary phase works better than a ternary one. A ternary system might end up with an internal porous nanowire. In any case, an extreme Kirkendall system, that is, where the outdiffusion of core material is significantly faster than the

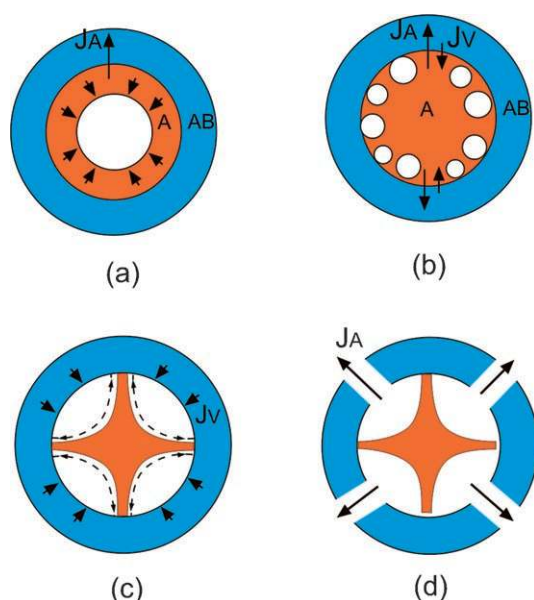


Figure 2. Different diffusion processes in the growth of hollow nanostructures induced by the Kirkendall effect. A stands for the core component and AB for the product phase. a) A continuous bulk diffusion of core and shell components through a continuous A/AB interface, and condensation of excess vacancies at the center of the core. b) At an early stage, small Kirkendall voids are generated via bulk diffusion at the interface. c) In a later stage, when the voids contact the inner surface of the product layer, the enlargement of the hollow core could be contributed by surface diffusion of atoms of the core material along the skeletal bridges. Reproduced with permission from Ref. [59]. d) If gaps are present in the shell layer, or appear during the growth, the material exchange can proceed via direct dissolution (in solution phase) or evaporation (in gas phase) through the gaps, leading to hollowing of the NPs.

inward diffusion of the shell phase, has a better chance of forming complete nanotubes. One explanation is that here the Kirkendall marker plane (r_K , an inert marker placed at the initial core/shell interface) lies at the interface of the core/product phase, so that all excess vacancies will accumulate at the periphery of r_K . However, in a normal binary system, or in a ternary system where the core material is an alloy (or compound) but only one element outdiffuses, the Kirkendall marker plane lies somewhere within the product phase. The only ternary-nanotube system demonstrated so far is ZnAl_2O_4 , formed through an interface reaction of $\text{ZnO}/\text{Al}_2\text{O}_3$ core/shell nanowires.^[46] This is not contradictory to Prasad and Paul's arguments, as the $\text{ZnO}/\text{Al}_2\text{O}_3$ reaction is effectively a one-way transfer of ZnO into alumina.^[56] Therefore, it can be considered as a pseudo binary case. The Kirkendall marker plane lies at the ZnO/spinel interface.

Tu and Gösele^[57] considered the Gibbs–Thomson effect in the thickening rate of the compound layer. The diffusion is then thermodynamically driven by the difference of the chemical potential of the atoms and the corresponding difference of equilibrium concentrations between the inner concave and outer convex surfaces. This gives an outward growth rate of

$$\frac{dr_{\text{out}}}{dt} \approx \frac{D_A}{kT} \left(-\frac{\Delta\mu}{r_{\text{out}} - r_{\text{in}}} \right) \quad (3)$$

where

$$\Delta\mu = \Delta G_{\text{reaction}} + 2\Omega \left(\frac{\gamma_{\text{out}}}{r_{\text{out}}} + \frac{\gamma_{\text{in}}}{r_{\text{in}}} \right) \quad (4)$$

where γ denotes the interface energy, Ω the atomic volume of A in the product phase, and $\Delta G_{\text{reaction}}$ is the formation energy of the product phase per atom. The notation deviates from Reference [57] in order to be consistent with Equation (1). Equation (3) implies that the direction of the reaction can be controlled by thermodynamics. For sufficiently small (i.e., large curvature) objects and high interface energies, this effect may counteract the concentration-driven diffusion in Equation (1) and, as a consequence, the formation of hollow structures is thermodynamically forbidden in the long run. In addition, pore formation can also be suppressed by applying an external pressure. Reasons for this is that the applied stress σ leads to a decrease in the pore size according to $\sigma = 2\gamma/r$, so that the excess vacancy concentration is lowered.

With the same thermodynamics argument as above, hollow nanoshells are unstable. Vacancies flow outward from the inner surface and are absorbed at the outer surface since the vacancy concentration at the inner surface $C_v^{\text{in}} = C_v^0 \exp(\frac{2\gamma\Omega}{kTr_{\text{in}}})$ is higher than that at outer surface $C_v^{\text{out}} = C_v^0 \exp(-\frac{2\gamma\Omega}{kTr_{\text{out}}})$. As a result, the spheres shrink and finally end up eliminating the empty space to minimize the interface energy. Gusak et al.^[58] showed in more detail that shrinkage is even more severe for single-element hollow nanospheres than compound ones, because of a “reverse Kirkendall effect” (atoms flow inward to compensate the outdiffusion of vacancies, which then reduce the vacancy flux) occurring in the later case. Reasonable approximations of the collapse time for both were given, for example, in the order of seconds for a gold nanoshell of $r_{\text{in}} = 3$ nm and $r_{\text{out}} = 6$ nm at 400 °C. Overall, the work by Tu et al.^[57] and Gusak et al.^[58] emphasizes the important role of thermodynamics in addition to kinetics in the evaluation of the nanoscale Kirkendall effect.

As a general conclusion of the available theoretical work, the formation of perfect hollow nano-objects is not a necessary result even when the diffusivity of core material exceeds that of the shell. Conditions preventing hollow core formation can be

- The specific geometry, diffusivity, and concentration profile do not satisfy Equation (2).
- The product phase is rich in defects, which may absorb vacancies without forming voids.
- It is a ternary mutual-diffusion system.
- The object is very small, which makes a hollow structure unstable in the given environment.

Choosing the right reaction temperature is important and should assure sufficient diffusivities of the atoms and vacancies. Otherwise, multiple voids could occur.

Previous discussions on Kirkendall-type diffusions consider a continuous bulk diffusion of the growth species and vacancies. Therefore, the pore enlarges only by aggregation of inward-flux excess vacancies at the center of the core (Figure 2a). However, in most real experiments, voids are generated near the interface and separate the core from the inner surface of the product layer, as observed by Yin et al.^[21] and Aldinger.^[22]

In this case, all above diffusion formulations become invalid. We proposed a conceptual extension based on our experimental observations,^[59] two main stages might be involved in the development of the hollow interior. The initial stage is the generation of small Kirkendall voids intersecting the product interface via a bulk diffusion process (Figure 2b); the second stage is dominated by surface diffusion of the core material (viz., the fast-diffusing species) along the pore surface (Figure 2c). As surface-diffusion coefficients are several orders of magnitude larger than their bulk counterpart, faster kinetics of the void growth is predicted. This concept should be generic, and applies to spherical as well as cylindrical nano- and microscale structures and even to macroscopic bilayers. Figure 3 shows examples of the Kirkendall voids developed at the film-substrate interfaces between a metallic alloy and a metal (Figure 3a)^[13] and between two compound materials (Figure 3b). Surface diffusion contributed to the growth of these big voids, as shown

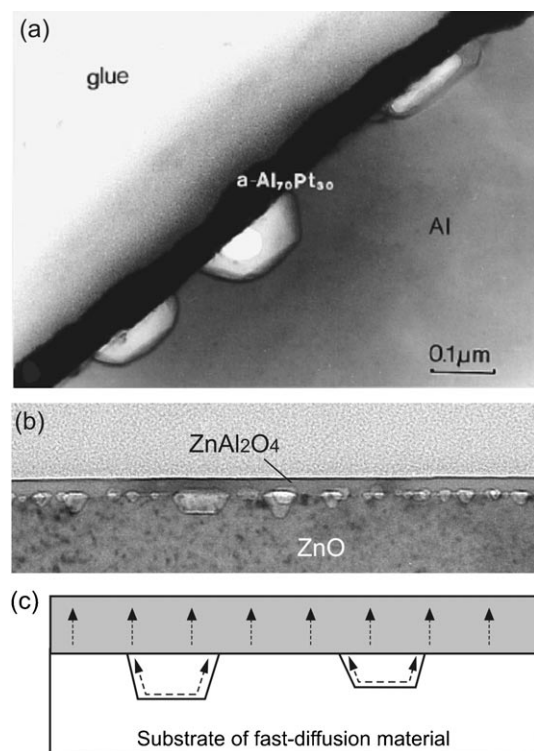


Figure 3. Voids at planar substrates based on the Kirkendall effect. a) Deposition of vapor Pt on an Al substrate, forming an amorphous alloy layer. b) Solid-solid reaction between ZnO substrate and a thin alumina film forming a ZnAl₂O₄ single-crystal layer. In both cases, some voids significantly larger than the rest are seen. Reproduced with permission from Ref. [59]. c) Schematics of the diffusion mechanism, highlighting the surface diffusion contribution. Reproduced with permission from Ref. [13].

schematically in Figure 3c. In fact, surface diffusion is the main mass-transport mechanism in powder sintering of metals and ceramics, which gives rise to coarsening and enhancement of pore growth,^[60–63] as well as in the elongation of carbon nanotubes^[64] and inorganic nanowires and nanotubes.^[65–67]

3. Hollow Nanoparticles

Aldinger^[22] was the first to study the hollowing of spherical particles induced by an extreme Kirkendall case early in 1974. Beryllium microparticles (of $\approx 33\text{-}\mu\text{m}$ diameter) were used as the starting material. The particles were coated with Co by evaporation or Ni by electroplating to form core/shell particles. Subsequent sintering produced a BeNi alloy shell with a partially hollow interior, resulting from a dominant outdiffusion of Be. In this microscopic system, excess vacancies annihilate at structure imperfections (such as edge dislocation and grain boundaries) at the core/shell interface, generating a radial stress. As a result of this stress cracks form and separate the core from the shell. This is why most of the resulting BeNi hollow particles have irregular skeletal remainders inside. The latter is an indication of the surface diffusion along the early formed pore walls. Recently reported ZnO hollow microcages by dry oxidation of Zn solid particles^[25,68] might follow a similar process as that in Aldinger's work: Zinc diffuses outward through the ZnO layer faster than oxygen inward, plus a strong surface diffusion along the pore/crack in the outer oxide layer (in addition to evaporation, of course, because of the high vapor pressure of Zn even at temperatures lower than its melting point of 420°C).

Coming to the nanoscale, due to the structural perfection and wide availability of single-crystal metal NPs, the Kirkendall effect can result in smooth and uniform-sized hollow compound nanocrystals. The Kirkendall effect originally comes from metal alloys but it now has embodiments in compound systems, mostly in oxides, sulfides, and nitrides, in which the oxidation, sulfidation, or nitridation of an elemental metal proceeds with a faster diffusion of the metal through the compounds (see Table 1). The first explicit example discussed was from the group of Alivisatos.^[21] Reaction of Co nanocrystals in solution in an elemental S or O₂/Ar ambient leads to the formation of hollow Co₃S₄ or CoO NPs, respectively. Particularly, a time-sequenced structure evolution gave strong evidence of the Kirkendall effect, as well as the implication of surface diffusions (see Figure 4a).^[54] The size of the final void was noticeably smaller than the initial Co NP, indicating an inward growth of the product shell. This is partly due to an inward transport of sulfur anions in addition to the predominant outdiffusion of Co cations. Gao et al.^[24] conducted an analogous experiment on Co NPs. The NPs were assembled via magnetic-dipole interaction into necklacelike structures and then reacted with Se and Te in solution, resulting in interconnected hollow NPs of crystalline CoSe₂ and CoTe (Figure 4b). Similarly, such a hollowing mechanism was implemented in many material systems. For example, Ni₂P and Co₂P hollow NPs

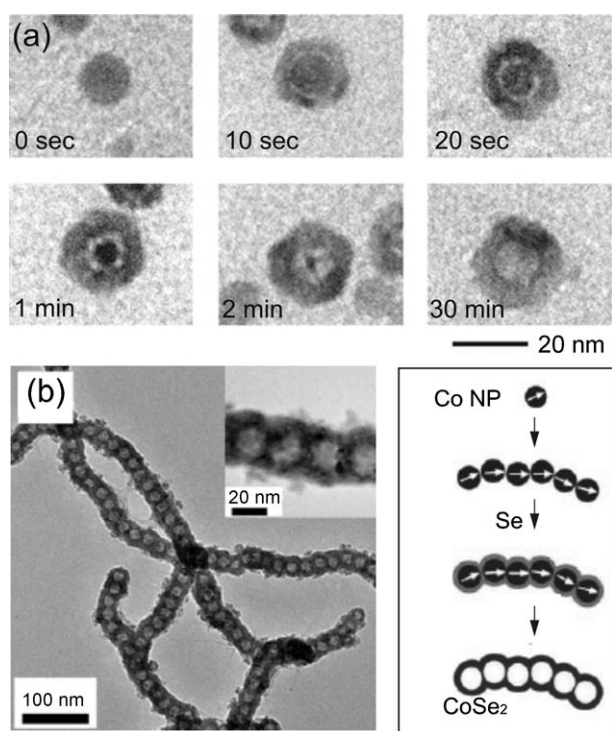


Figure 4. Examples of hollow nanocrystals formed through the nanoscale Kirkendall effect. a) TEM images showing the development of voids in a time-sequenced reaction of colloidal Co NPs with sulfur leading to cobalt sulfide hollow nanocrystals. Reproduced with permission from Ref. [21]. b) Chain of CoSe_2 nanocrystals by solution reaction of the wired Co NPs with Se. The corresponding mechanism is shown in the right-hand column. The initial Co NPs were assembled into a necklace structure due to magnetic-dipole interaction. Reproduced with permission from Ref. [24].

through a retarded phosphidation of the corresponding metal NPs in solution by trioctylphosphine (TOP).^[38] A reaction of Pb NPs with sulfur vapor resulted in hollow PbS ,^[29] whereas an oxidation ended up with solid PbO NPs, as the diffusivity of oxygen is actually larger than that of Pb at the Pb/ PbO interface.^[27] The Kirkendall mechanism holds even for microscale objects such as MoS_2 microcages^[36] and MoO_2 microspheres,^[37] regardless of the fabrication details.

A special Kirkendall process is the low-temperature oxidation of metal NPs such as Fe, Zn, and Al.^[27,33,34] Oxidation of these metal NPs of a size below a critical value (8 nm for Fe at 300 K, 8 nm for Al at 423 K, and 20 nm for Zn at 423 K) leads to hollow oxide nanospheres. However, for metal NPs larger than the critical size, voids are not observed; instead, they turned to metal/oxide core/shell solid spheres with their oxide thicknesses independent of the initial particle size and oxidation time. The void formation of the small metal NPs characterizes the low-temperature, early oxidation behavior of metals. In this case, the fast outward diffusion of metal cations was not thermally activated but driven by an electric field built between the metal and an initial thin oxide layer (≈ 3 nm) at the beginning, according to the Cabrera–Mott theory.^[69]

In addition to the reaction of a single element to a compound, another strategy is to convert one compound into

another, which involves diffusions of different rates during a substitution reaction. For example, reaction of solid ZnO nanospheres or nanobelts with H_2S water results in porous ZnS cages and tubes, respectively.^[28,70] Similarly, solid templates of CuO and CuCl can also be converted to CuS hollow nanostructure by sulfidation, giving rise to hollow cages and nanotubes.^[30,31,53]

Reasonably, from an experimental point of view, in order to obtain pure-phase hollow nanocrystals, there should be a suitable amount of shell material relative to the starting crystals. In light of this, reaction in a vapor or solution phase is more favorable than a solid–solid reaction since under the former conditions the supply of the shell material is constant and sufficient. Demonstrated examples include dry sulfidation of Pb nanocrystals^[29] and Cd nanowires,^[46] wet sulfidation of Co nanocrystals,^[21] and dry oxidation of Cu nanowires.^[52]

Moreover, although unnoted by the authors, the Kirkendall effect might have also been the driving force for formation of some other hollow nanocrystals. For example, gold^[23] and AuPt bimetallic^[35] nanoshells were synthesized in solution. Prospectively, nitridation of a solid Si NP should lead to a Si_3N_4 hollow sphere, since nitridation of a silicon thin film leads to vacancy injection due to a faster diffusion of the silicon than the nitrogen within Si_3N_4 .^[71] However, oxidation of Si NPs through the normal oxygen diffusion and reaction at the silicon/oxide interface does not lead to a hollow oxide sphere. It is even worse if one takes into account the retardation effect observed for curved Si surfaces, because here one has an increased stress at the silicon/oxide interface of such a large curvature.^[72,73] Contrary to this theoretical expectation the following phenomenon was reported by Colder et al.:^[43] solid Si NPs (≈ 12 nm in diameter) were aged in water for two days followed by a moderate heating (120 – 140°C) and found to be transformed into hollow spherical SiO_2 NPs. This gives a hint that the thermal oxidation of silicon in water at low temperatures behaves differently to the normally accepted process. A possible overall Si outdiffusion process might be as follows: some oxygen-containing species such as OH^- diffuse through the oxide to the Si/oxide interface, react with the core, and form a silicon-containing species such as SiO^- , which outdiffuses to the oxide surface and reacts with H_2O forming SiO_2 plus hydrogen. If proved, such combination of interdiffusion and two solution reactions represents a process analogous to the Kirkendall effect. Alternatively, an electric-field-driven process for very thin oxides analogous to that suggested by Cabrera and Mott^[69] might have to be considered.

The advantage of the Kirkendall method for fabricating hollow NPs is as follows. The most widely adopted method is to use commercially available polystyrene and silica spheres as the sacrificial template. Because of the intrinsic size limit of the polystyrene or silica spheres, this route generally results in large hollow structures in the submicrometer range. Colloidal metal nanocrystals (Au, Pt, Pd, etc.) can be chemically synthesized with a high yield, and their reactions with suitable materials in combination with the Kirkendall-type diffusion can give rise to highly crystalline hollow NPs even in the quantum regime. Furthermore, com-

pared to many multistep organic chemical fabrication routes, which usually need further purification processes, the Kirkendall method is a one-pot mass synthesis with a nearly 100% purity.

4. Nanotubes

The Kirkendall-based fabrication route has also been extended to tubular structures.^[46–53] The experimental strategies for nanotubes have been partly mentioned in the previous section. Here we will stress issues on specific diffusion and growth processes in the case of nanotubes. Different from spherical NPs, which correspond to a quasi zero-dimensional (0D) system and isotropic void growth, the nanotubes have one more degree of freedom and allow material transport along the longitudinal axes. This can result in an uneven growth of the voids and hence, when the core material exceeds the shell material coated for reaction, segmented tubes, which are partly hollow and partly solid.^[59] Another possibility is the void growth from both ends of the solid nanowire template by a mediated diffusion of the core material on its end faces.^[49]

We demonstrated a fabrication route to monocrystalline ZnAl_2O_4 spinel nanotubes based on the Kirkendall effect, as shown in Figure 5a. Pre-synthesized ZnO nanowires (10–30 nm thick, up to 20 μm long) were coated with a 10-nm-thick conformal layer of alumina via atomic-layer deposition (ALD) at 200 °C. The thus formed ZnO/ Al_2O_3 core/shell nanowires were annealed in air at 700 °C for 3 h, causing an interfacial solid-state reaction and diffusion. Because the reaction is effectively a one-way transfer of ZnO into alumina,^[56] it represents a case of the extreme Kirkendall effect. Figure 5b and c shows transmission electron microscopy

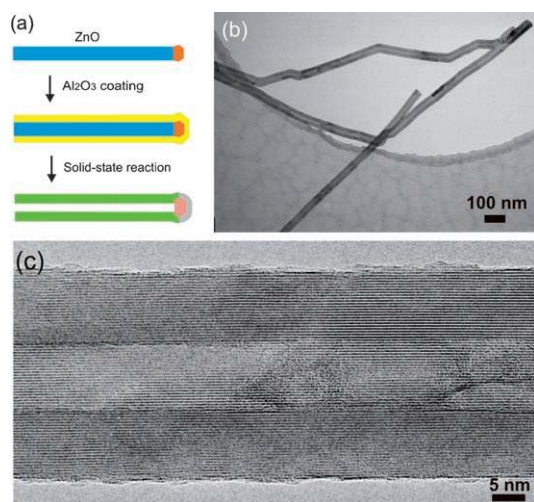


Figure 5. Crystalline spinel ZnAl_2O_4 nanotube through interface solid-state reaction of ZnO/ Al_2O_3 core/shell nanowires involving the Kirkendall-type diffusion. a) Schematic images of the fabrication process. Coating of a conformal alumina layer was done by atomic layer deposition. b) TEM image of several nanotubes. c) High-resolution TEM image of the tube wall. Reproduced with permission from Ref. [47].

(TEM) images of the resulting ZnAl_2O_4 spinel nanotubes. Here, the conformity and uniformity characteristics of ALD are essential to the formation of smooth nanotubes. Other coating methods, such as sputtering or vapor deposition,^[50,74] are expected to result in nonuniformity, rugged surface, or mixed phase of the tube wall.

These ternary compound nanotubes by the Kirkendall route are more stable than the nanotubes of barium and strontium titanate^[75] by rolling up of the initial sheets, and the nanotubes produced in hydrothermal reactions like titanium phosphate^[76] and uranyl selenate.^[77] Note that the Zn_2SiO_4 nanotubes formed through the solid-state reaction of ZnO/Si core/shell nanorods^[50] might also involve a Kirkendall diffusion process analogous to that in Figure 5.

In the experiment in which Ag nanowires were converted into polycrystalline Ag_2Se nanotubes,^[49] the reaction was surface mediated by surfactants so that the voids were observed to grow horizontally along the wire axis rather than isotropically (see Figure 6). This was related to a controlled

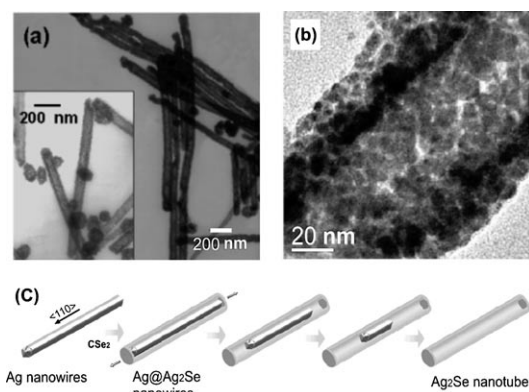


Figure 6. Ag_2Se nanotubes formed based on the Kirkendall effect. a) TEM image of the tubes. b) Higher-magnification view of the tube showing that the tube wall is composed of multiple grains. c) Schematic images of the diffusion process. Due to the higher concentration of CSe_2 adsorbed at the end (111) faces than on the side (100) faces of the Ag nanowires, the void grows along the longitudinal $\langle 110 \rangle$ direction from the ends. Reproduced with permission from Ref. [49].

preferential adhesion of CSe_2 , the other reactant, on the ends of the Ag nanowire rather than on its side faces. Hence, the high concentration of Se atoms at the nanowire ends promotes the diffusion of Ag^+ along the longitudinal axis, leading to the observed anisotropic growth of vacancies along $\langle 110 \rangle$ (see Figure 6c). This represents a different strategy of applying the Kirkendall effect to nanotube formation from the one presented in Figure 5.

Aforementioned are free-standing nanotubes. Horizontally aligned (relative to the substrate surface) tubular structures can also be formed by the same mechanism. Li and Penner^[46] fabricated ultralong, parallel, hemicylindrical CdS nanoshells by reacting the electrochemically deposited Cd nanowires with H_2S vapor (see Figure 7). Although these nanoshells might not yet be readily used for nanofluidic applications, because of their rugged inner surface and polycrystalline nature, it demonstrates the concept.

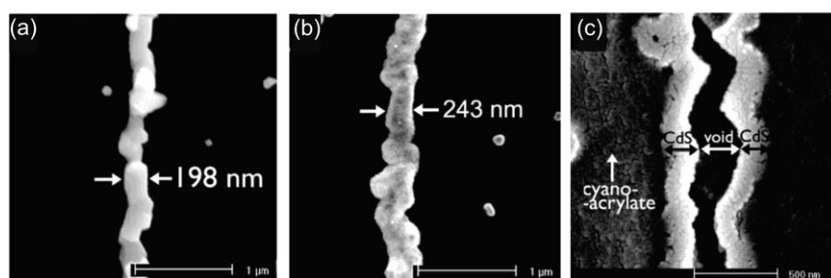


Figure 7. Conversion of horizontally aligned Cd nanowires into hemicylindrical CdS nanoshells induced by the Kirkendall effect. a) SEM image of one Cd nanowire through electrochemical step-edge decoration on a graphite electrode surface. b) Corresponding CdS hemicylindrical nanoshell by converting the Cd nanowires into CdS by exposure to gaseous H_2S at elevated temperature. c) The CdS nanoshell was transferred from the initial conductive graphite surface to a cyanoacrylate-coated glass surface, revealing the surface of the nanowire that was previously in contact with the graphite surface. Reproduced with permission from Ref. [46].

One important issue for the formation of perfect nanotubes (as well as hollow NPs) is that an initial “insulating” layer is practically mandatory. This was pointed out by several authors in their solution-phase synthesis of hollow structures induced by the Kirkendall effect.^[26,49,52,53] Formed at the early stage of the reaction, this insulating layer prevents a direct penetration or evaporation of the reactant and hence establishes a *solid* diffusion medium. Without this layer, or in case of an incontinuous layer (with gaps),

nanowires react with a vapor phase of the other species, which leads to an uneven deposition and a local aggregation on the nanowire surface. Therefore, large gaps are available for surface diffusion of ZnO. Furthermore, gaps can form during the reaction process due to lattice-mismatch-induced stress or shell deformation. An example for the former is the dry oxidation of Zn polyhedra microparticles, where gaps were produced in a thin outer ZnO layer especially in the basal plane (lattice mismatch 23.7%).^[25,68] The latter

was observed for the reaction of Co NPs with sulfur.^[54] Overall, a hollowing process in many circumstances might be a combination of various material transport mechanisms (Figure 2).

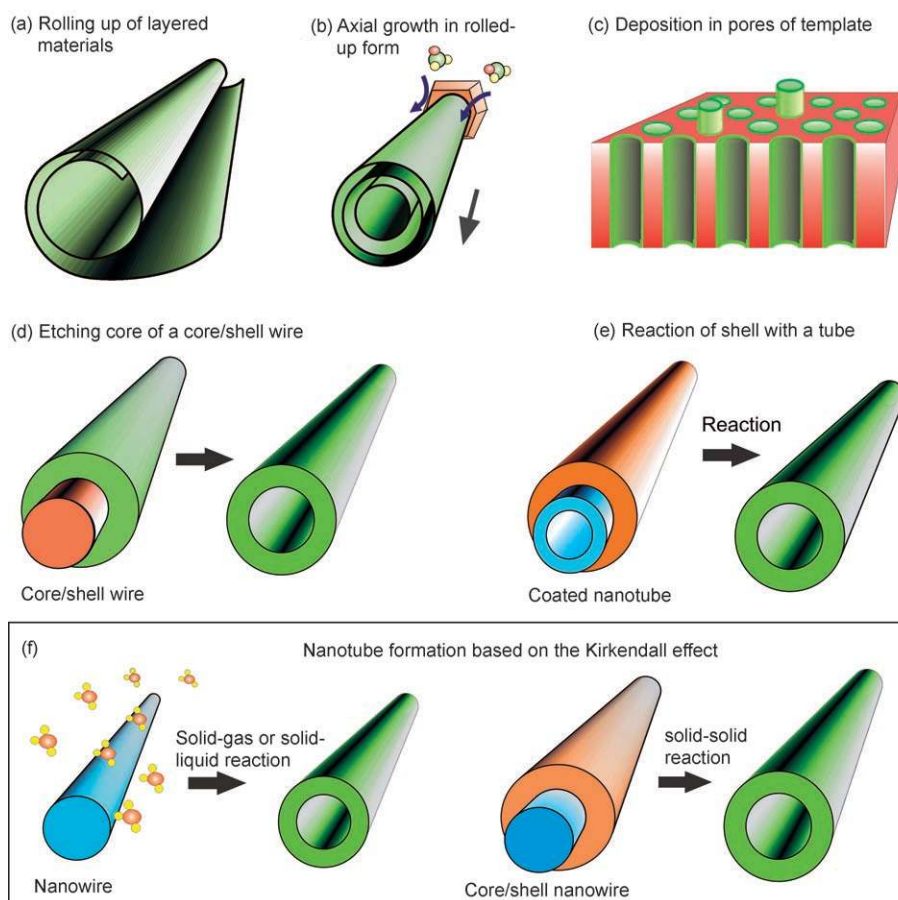


Figure 8. A summary of the principal methods for nanotube synthesis. See text for details. Reproduced with permission from Ref. [47].

4.1 Comparison to Other Nanotube Fabrication Routes

In this section, we summarize the common fabrication routes to nanotubes and compare them to the Kirkendall method. Figure 8 gives a schematic summary of typical approaches to generate composite nanotubes. They can be classified into the following categories:

- 1) Layered materials rolled up to form nanoscrolls, for instance, semiconductor thin films rolled up by strain release of the lattice-mismatched film-substrate interface,^[80] and graphite can roll up by intercalation exfoliation.^[81]

- 2) Layered materials grow in a rolled-up fashion, starting from a metal catalyst particle or a nuclei, and elongate axially by a reaction at the tip or at the root. This is similar to the growth of multi-walled (MW) CNTs, and applies mainly to the fullerene-like inorganic nanotubes.^[5]
- 3) Deposition in a porous template (anodic alumina, zeolites, etc.) via precursor infiltration/wetting,^[82] electrochemical decoration,^[83] or ALD,^[84] followed by template removal.
- 4) Eliminating the core of a preformed core/shell nanowire by etching, evaporation, or dissolution.^[85–87]
- 5) Reaction of a nanotube with a shell material or solvent to form complex compositions.^[75]
- 6) Transformation of a solid nanowire through interface reactions involving the Kirkendall effect. Nanoscrolls formed by method (1) are usually less stable than nanotubes. Method (3) is a common route for producing large-aspect-ratio (>100) nano- or microtubes but the drawback is that the tubes are in most cases polycrystalline. The merits of the Kirkendall-based method are as follows:
 - i) It is template-free and needs no layered materials, while being capable of producing large-aspect-ratio tubes.
 - ii) It is anticipated to work with both binary and ternary and even more complicated systems, based on the proper choice of materials and different reaction properties that are well known from thin-film diffusion couples. The Kirkendall-based method for ternary compound nanotubes is of particular interest. The resulting nanotubes can be single crystals,^[47,50,53] which is a major improvement compared to the usual polycrystalline nanotubes by pore wetting (Figure 8c). Also, they are more stable than ternary nanotubes by scrolling up of sheets (mechanism in Figure 8a) or those produced in hydrothermal reactions (mechanism in Figure 8e).^[75,76]
 - iii) The recent advance in fabrication and manipulation of single-crystalline nanowires of a wide spectrum of materials (both metals and semiconductors)^[88] allows a rational design of tubular structures. As the template is sacrificed no additional template removal procedure is needed.

This enables, for example, a segmental hollowing by selective exposure of the nanowire to the reactants. Also, free-standing and vertically aligned nanotubes arrays (such as the well-known CNTs arrays) by using well-ordered nanowires would be possible.^[89] For example, an array of zinc spinel nanotubes starting from ordered ZnO nanowires,^[90] or horizontally aligned channels using parallel arrays of metal nanowires, as in the case of CdS hemicylindrical nanoshells.^[46] Going further, when the nanowires are post-growth assembled, application of the Kirkendall-based method could then lead to hierarchical tubular structures, for example, branched channels when starting with crossed-linked nanowires, which is interesting for applications in nanofluidics. In such a way, physical or etching damage to the nanotubes, which may occur during post-growth assembly of nanotubes, could be avoided.

4.2 Nanotubes Formed by Other Diffusion Reactions

In this section, we will focus on inorganic nanotubes based on interface reaction and diffusion processes on a solid nanowire template, followed by removal of the remaining wire body to form the hollow core. The associated diffusion process can be a mutual diffusion with equal diffusivity, or one-way inward diffusion. Therefore, the hollowing is not directly due to the Kirkendall effect.

Possibly the most simple system is the thermal oxidation of Si nanowires in an oxygen environment, in which oxygen diffuses inward and reacts at the interface of Si and an oxide. Upon etching away the remaining Si core, a nanotube of the oxide shell will be obtained. Fan et al.^[91] demonstrated this idea using vertically aligned Si nanowire arrays and successively etched the gold tip, silica cap, and silicon core, eventually leaving a vertically aligned array of silica nanotubes. (It is noteworthy that, compared to this tedious procedure, a facile method for silica nanotubes of a controllable tube-wall thickness was reported by using ZnO nanowire templates and diffusive etching.^[92]) Even simpler, recalling the unusual oxidation behavior of silicon NPs in water,^[43] it

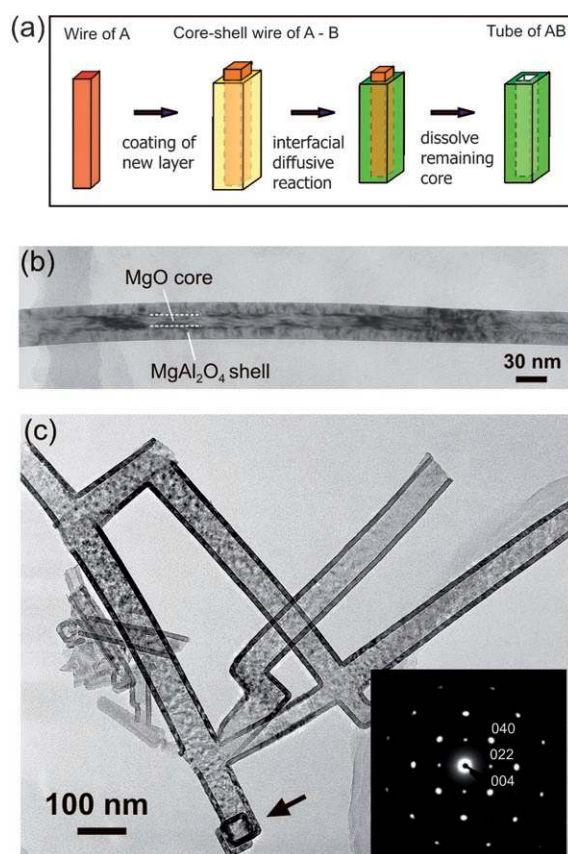


Figure 9. Spinel MgAl_2O_4 nanotubes based on reaction and Wagner cation counterdiffusion. a) Schematic images of the fabrication process. b) TEM image of one $\text{MgO}/\text{MgAl}_2\text{O}_4$ core/shell nanowire. c) TEM image of a complicated nanotube web of spinel MgAl_2O_4 . The arrow indicates the square cross section of the nanotubes. Inset is the corresponding electron diffraction pattern revealing the single crystallinity. Reproduced with permission from Ref. [93].

is anticipated that an analogous water oxidation of thin silicon nanowires might also lead to silica nanotubes.

A solid-state reaction occurring during the ceramics sintering involves various types of diffusion processes (bulk, surface, or grain-boundary diffusion) and mechanisms (cation counterdiffusion, or cation–anion joint diffusion). Implementation of the solid-state reaction using nanowires as one reactant provides a method for rational synthesis of compound oxide nanotubes. Examples are the spinel MgAl_2O_4 (ZnFe_2O_4) nanotubes^[93] using single-crystal MgO (ZnO) nanowires as the “substrate”. The nanowires were then coated with a conformal layer of alumina (Fe_2O_3) via ALD. The interface solid-state reaction took place upon annealing the core/shell nanowires at 700–800 °C under ambient conditions, during which cation pairs (Mg^{2+} and Al^{3+} , or Zn^{2+} and Fe^{3+}) diffuse in opposite directions while the oxygen sublattice is fixed. This is the well-known Wagner counterdiffusion mechanism. As the core nanowire has a larger diameter than necessary for a complete spinel reaction with the ALD shell, part of the core remains and can be etched in an ammonia sulfuric (in the case of MgO) or diluted HCl solution (in the case of ZnO). Spinel nanotubes of single-crystalline walls can thus be obtained. Figure 9 shows the fabrication process of the MgAl_2O_4 spinel nanotubes and the TEM images corresponding to selected stages. This method could be extended to other MgO- or ZnO-based spinel oxides when the MgO or ZnO nanowires are coated with other ALD-processable oxides (such as In_2O_3 , SnO_2 , TiO_2 , or Cr_2O_3), or with vapors of the oxide materials generated by electron-beam evaporation or pulsed-laser ablation. When doped, the spinel nanotubes might have applications in phosphor and magnetic devices.

5. Conclusions and Outlook

Conventionally, the Kirkendall effect, in combination with void formation, has been considered as a negative phenomenon degrading the integrity of interfaces. Here we have shown that, in contrast, on the nanoscale, the Kirkendall effect may be used positively to fabricate designed hollow nanostructures. We have summarized all the examples demonstrated to date in two categories: hollow nanoparticles and nanotubes. We discussed the practical requirements and the impact of specific growth mechanisms. We suggested that the Kirkendall effect might be a generic fabrication route to a diverse range of hollow nanostructures. For nanotube fabrication, we compared the Kirkendall method to other common fabrication methods and proposed its merits particularly for nanofluidic applications and ternary compound synthesis. It was also pointed out that the pore formation might be induced by the Kirkendall effect only at the beginning while its later-stage growth may result from other mechanisms such as surface diffusion along the pore walls or a direct elapse of core material through gaps in the shell.

Recent theoretical work was reviewed and evaluated in terms of how the thermodynamics and kinetics can differ from those in bulk systems, and under what circumstances a

hollow nanostructure will or will not be formed. The real diffusion processes on the nanoscale can be complicated by many factors. All the theoretical conclusions based on a steady-state assumption might be unreliable in terms of, for example, growth rate and time needed for a complete hollow core. Computer simulations of nanoscale Kirkendall processes might be favored in terms of including more complex phenomena and of accuracy.

Acknowledgements

The authors appreciate stimulating discussions with D. Hesse, R. Scholz, M. Knez, K. Nielsch, and E. Pippel.

- [1] H. W. Kroto, J. R. Heath, S. C. O'Brien, R. F. Curl, R. E. Smalley, *Nature* **1985**, 318, 162.
- [2] S. Iijima, *Nature* **1991**, 354, 56.
- [3] a) R. Tenne, L. Margulis, M. Genut, G. Hodes, *Nature* **1992**, 360, 444; b) L. Margulis, G. Salitra, R. Tenne, M. Talianker, *Nature* **1993**, 365, 113.
- [4] M. Terrones, J. M. Romo-Herrera, E. Cruz-Silva, F. López-Urías, E. Muñoz-Sandoval, J. J. Velázquez-Salazar, H. Terrones, Y. Bando, D. Golberg, *Mater. Today* **2007**, 10, 30.
- [5] a) R. Tenne, *Angew. Chem.* **2003**, 115, 5280–5289; *Angew. Chem. Int. Ed.* **2003**, 42, 5124; b) R. Tenne, *Nat. Nanotechnol.* **2006**, 1, 103.
- [6] H. C. Zeng, *J. Mater. Chem.* **2006**, 16, 649.
- [7] Y. Xiong, B. T. Mayers, Y. Xia, *Chem. Commun.* **2005**, 5013.
- [8] J. Goldberger, R. Fan, P. D. Yang, *Acc. Chem. Res.* **2006**, 39, 239.
- [9] a) E. O. Kirkendall, *Trans. AIME* **1942**, 147, 104; b) A. D. Smigelskas, E. O. Kirkendall, *Trans. AIME* **1947**, 171, 130.
- [10] H. Nakajima, *J. Miner. Met. Mater. Soc.* **1997**, 49, 15.
- [11] A. Paul, PhD thesis, Technische Universiteit Eindhoven, The Netherlands, **2004**.
- [12] H. Schröder, K. Samwer, U. Köster, *Phys. Rev. Lett.* **1985**, 54, 197.
- [13] Z. Radi, P. B. Barna, J. Labar, *J. Appl. Phys.* **1996**, 79, 4096.
- [14] K. Zeng, R. Stierman, T.-C. Chiu, D. Edwards, K. An, K. N. Tu, *J. Appl. Phys.* **2005**, 97, 024508.
- [15] A. Seeger, K. P. Chik, *Phys. Stat. Sol.* **1968**, 29, 455.
- [16] H. Bracht, *Nucl. Instrum. Methods Phys. Res. Sect. B* **2006**, 253, 105.
- [17] U. Gösele, H. Strunk, *Appl. Phys. A* **1979**, 20, 265.
- [18] D. L. Anton, A. G. Giamei, *Mater. Sci. Eng.* **1985**, 76, 173.
- [19] D. Tomus, K. Tsuchiya, M. Inuzuka, M. Sasaki, D. Imai, T. Ohmori, M. Umemoto, *Scr. Mater.* **2003**, 48, 489.
- [20] J. D. Kelen, G. Warshaw, N. Duziak, S. F. Cogan, R. M. Rose, *IEEE Trans. Magn.* **1981**, 17, 380.
- [21] Y. Yin, R. M. Rioux, C. K. Erdonmez, S. Hughes, G. A. Somorjai, A. P. Alivisatos, *Science* **2004**, 304, 711.
- [22] F. Aldinger, *Acta Metal.* **1974**, 22, 923.
- [23] Y. Sun, Y. Xia, *Science* **2002**, 298, 2176.
- [24] J. H. Gao, B. Zhang, X. X. Zhang, B. Xu, *Angew. Chem.* **2006**, 118, 1242–1245; *Angew. Chem. Int. Ed.* **2006**, 45, 1220.
- [25] H. J. Fan, R. Scholz, F. M. Kolb, M. Zacharias, U. Gösele, *Solid-State Commun.* **2004**, 130, 517.
- [26] B. Liu, H. C. Zeng, *J. Am. Chem. Soc.* **2004**, 126, 16744.
- [27] R. Nakamura, D. Tokozakura, H. Nakajima, J. G. Lee, H. Mori, *J. Appl. Phys.* **2007**, 101, 074303.
- [28] H. F. Shao, X. F. Qian, Z. K. Zhu, *J. Solid State Chem.* **2005**, 178, 3522.
- [29] Y. Wang, L. Cai, Y. Xia, *Adv. Mater.* **2005**, 17, 473.

- [30] H. L. Xu, W. Z. Wang, W. Zhu, L. Zhou, *Nanotechnology* **2006**, 17, 3649.
- [31] H. L. Cao, X. F. Qian, C. Wang, X. D. Ma, J. Yin, Z. K. Zhu, *J. Am. Chem. Soc.* **2005**, 127, 16024.
- [32] L. Z. Zhang, J. C. Yu, Z. Zheng, C. W. Leung, *Chem. Commun.* **2005**, 2683.
- [33] C. M. Wang, D. R. Baer, L. E. Thomas, J. E. Amonette, J. Antony, Y. Qiang, G. Duscher, *J. Appl. Phys.* **2005**, 98, 094308.
- [34] R. Nakamura, J. G. Lee, D. Tokozakura, H. Mori, H. Nakajima, *Mater. Lett.* **2007**, 61, 1060.
- [35] H. P. Liang, Y. G. Guo, H. M. Zhang, J. S. Hu, L. J. Wan, C. L. Bai, *Chem. Commun.* **2004**, 1496.
- [36] L. N. Ye, C. Z. Wu, W. Guo, Y. Xie, *Chem. Commun.* **2006**, 4738.
- [37] C. H. Guo, G. J. Zhang, Z. R. Shen, P. C. Sun, Z. Y. Yuan, Q. H. Jin, B. H. Li, D. T. Ding, T. H. Chen, *Chinese J. Chem. Phys.* **2006**, 19, 543.
- [38] P. K. Chiang, R. T. Chiang, *Inorg. Chem.* **2007**, 46, 369.
- [39] J. H. Gao, G. L. Liang, B. Zhang, Y. Kuang, X. X. Zhang, B. Xu, *J. Am. Chem. Soc.* **2007**, 129, 1428.
- [40] S. H. Zhou, B. Varughese, B. Eichhorn, G. Jackson, K. McIlwrath, *Angew. Chem.* **2005**, 117, 4615; *Angew. Chem. Int. Ed.* **2005**, 44, 4539.
- [41] Y. W. Ma, K. F. Huo, Q. Wu, Y. N. Lu, Y. M. Hu, Z. Hu, Y. Chen, *J. Mater. Chem.* **2006**, 16, 2834.
- [42] J. Zheng, X. B. Song, Y. H. Zhang, Y. Li, X. G. Li, Y. K. Pu, *J. Solid State Chem.* **2007**, 180, 276.
- [43] A. Colder, F. Huisken, E. Trave, G. Ledoux, O. Guillois, C. Reynaud, H. Hofmeister, E. Pippel, *Nanotechnology* **2004**, 15, L1.
- [44] Y. G. Li, B. Tan, Y. Y. Wu, *J. Am. Chem. Soc.* **2006**, 128, 14258.
- [45] Y. W. Wang, H. Xu, X. B. Wang, X. Zhang, H. M. Jia, L. Z. Zhang, J. R. Qiu, *J. Phys. Chem. B* **2006**, 110, 13835.
- [46] Q. Li, R. M. Penner, *Nano Lett.* **2005**, 5, 1720.
- [47] H. J. Fan, M. Knez, R. Scholz, K. Nielsch, E. Pippel, D. Hesse, M. Zacharias, U. Gösele, *Nat. Mater.* **2006**, 5, 627.
- [48] H. Tan, S. P. Li, W. Y. Fan, *J. Phys. Chem. B* **2006**, 110, 15812.
- [49] C. H. B. Ng, H. Tan, W. Y. Fan, *Langmuir* **2006**, 22, 9712.
- [50] J. Zhou, J. Liu, X. D. Wang, J. H. Song, R. Tummala, N. S. Xu, Z. L. Wang, *Small* **2007**, 3, 622.
- [51] X. Y. Chen, Z. J. Zhang, Z. G. Qiu, C. W. Shi, X. L. Li, *J. Colloid Interface Sci.* **2007**, 308, 271.
- [52] Y. Chang, M. L. Lye, H. C. Zeng, *Langmuir* **2005**, 21, 3746.
- [53] Q. Wang, J. X. Li, G. D. Li, X. J. Cao, K. J. Wang, J. S. Che, *J. Cryst. Growth* **2007**, 299, 386.
- [54] Y. Yin, C. K. Erdonmez, A. Cabot, S. Hughes, A. P. Alivisatos, *Adv. Funct. Mater.* **2006**, 16, 1389.
- [55] S. Prasad, A. Paul, *Appl. Phys. Lett.* **2007**, 90, 233114.
- [56] a) B. Bengtson, R. Jagitsch, *Arkiv Kemi, Mineral. Geol.* **1947**, 24A, 1; b) D. L. Branson, *J. Am. Ceram. Soc.* **1965**, 48, 591.
- [57] K. N. Tu, U. Gösele, *Appl. Phys. Lett.* **2005**, 86, 093111.
- [58] A. M. Gusak, T. V. Zaporozhets, K. N. Tu, U. Gösele, *Philos. Mag.* **2005**, 85, 4445.
- [59] H. J. Fan, M. Knez, R. Scholz, D. Hesse, K. Nielsch, M. Zacharias, U. Gösele, *Nano Lett.* **2007**, 7, 993.
- [60] G. C. Kuczynski, *Trans. AIME* **1949**, 185, 169.
- [61] O. J. Whittemore, J. A. Varela, *J. Am. Ceram. Soc.* **1981**, 64, C154.
- [62] A. Akash, M. J. Mayo, *J. Am. Ceram. Soc.* **1999**, 82, 2948.
- [63] J. P. Han, P. Q. Mantas, A. M. R. Senos, *J. Am. Ceram. Soc.* **2005**, 88, 1773.
- [64] O. A. Louchev, H. Kanda, A. Rosén, K. Bolton, *J. Chem. Phys.* **2004**, 121, 446.
- [65] R. Scholz, U. Gösele, E. Niemann, D. Leidich, *Appl. Phys. Lett.* **1995**, 67, 1453.
- [66] O. A. Louchev, *Appl. Phys. Lett.* **1997**, 71, 3522.
- [67] L. Schubert, P. Werner, N. D. Zakharov, G. Gerth, F. M. Kolb, L. Long, U. Gösele, T. Y. Tan, *Appl. Phys. Lett.* **2004**, 84, 4968.
- [68] P. X. Gao, Z. L. Wang, *J. Am. Chem. Soc.* **2003**, 125, 11299.
- [69] N. Cabrera, N. F. Mott, *Rep. Prog. Phys.* **1949**, 12, 163.
- [70] X. Wang, P. X. Gao, J. Li, C. J. Summer, Z. L. Wang, *Adv. Mater.* **2002**, 14, 1732.
- [71] T. Y. Tan, U. Gösele, *Appl. Phys. A* **1985**, 37, 1.
- [72] D. B. Kao, J. P. , McVittie, W. D. Nix, K. C. Saraswat, *IEEE Trans. Electron Devices* **1987**, 34, 1008.
- [73] C. C. Büttner, M. Zacharias, *Appl. Phys. Lett.* **2006**, 89, 263106.
- [74] Y. J. Li, M. Y. Lu, C. W. Wang, K. M. Li, L. J. Chen, *Appl. Phys. Lett.* **2006**, 88, 143102.
- [75] Y. Mao, S. Banerjee, S. S. Wong, *Chem. Commun.* **2003**, 408.
- [76] Z. Yin, Y. Sakamoto, J. Yu, S. Sun, O. Terasaki, R. Xu, *J. Am. Chem. Soc.* **2004**, 126, 8882.
- [77] S. V. Krivovichev, V. Kahlenberg, R. Kaindl, E. Mersdorf, I. G. Tananaev, B. F. Myasoedov, *Angew. Chem.* **2004**, 117, 1158; *Angew. Chem. Int. Ed.* **2004**, 44, 1134.
- [78] X. Wang, C. J. Summers, Z. L. Wang, *Adv. Mater.* **2004**, 16, 1215.
- [79] H. J. Fan, A. Lotnyk, R. Scholz, Y. Yang, D. S. Kim, E. Pippel, S. Senz, D. Hesse, M. Zacharias, unpublished results.
- [80] a) V. Ya. Prinz, V. A. Seleznev, A. K. Gutakovskiy, A. V. Chehovskiy, V. V. Preobrazhenskii, M. A. Putyato, T. A. Gavrilova, *Phys. E* **2000**, 6, 828; b) O. G. Schmidt, K. Eberl, *Nature* **2001**, 410, 168; c) O. G. Schmidt, N. Schmarje, C. Deneke, C. Müller, N. Y. Jin-Phillipp, *Adv. Mater.* **2001**, 13, 756.
- [81] L. M. Viculis, J. J. Mack, R. B. Kaner, *Science* **2003**, 299, 1361.
- [82] a) M. Steinhart, R. B. Wehrspohn, U. Gösele, J. H. Wendorff, *Angew. Chem.* **2004**, 116, 1356; *Angew. Chem. Int. Ed.* **2004**, 43, 1334; b) L. Zhao, T. Z. Lu, M. Zacharias, J. Yu, J. Shen, H. Hofmeister, M. Steinhart, U. Gösele, *Adv. Mater.* **2006**, 18, 363; c) F. D. Morrison, L. Ramsay, J. F. Scott, *J. Phys. Condens. Matter* **2003**, 15, L527.
- [83] W. Lee, R. Scholz, K. Nielsch, U. Gösele, *Angew. Chem.* **2005**, 117, 6204; *Angew. Chem. Int. Ed.* **2005**, 44, 6050.
- [84] a) H. Shin, D. K. Jeong, J. Lee, M. M. Sung, J. Kim, *Adv. Mater.* **2004**, 16, 1197; b) M. Daub, M. Knez, U. Gösele, K. Nielsch, *J. Appl. Phys.* **2007**, 101, 09J111; c) J. Bachmann, J. Jing, M. Knez, S. Barth, H. Shen, S. Mathur, U. Gösele, K. Nielsch, *J. Am. Chem. Soc.*, **2007**, 129, 9554.
- [85] J. Goldberger, R. He, Y. F. Zhang, S. Lee, H. Q. Yan, H. J. Choi, P. Yang, *Nature* **2003**, 422, 599.
- [86] R. H. A. Ras, M. Kemell, J. de Wit, M. Ritala, G. ten Brinke, M. Leskelä, O. Ikkala, *Adv. Mater.* **2007**, 19, 102.
- [87] G. Z. Shen, Y. Bando, C. H. Ye, X. L. Yuan, T. Sekiguchi, D. Golberg, *Angew. Chem.* **2006**, 118, 7730; *Angew. Chem. Int. Ed.* **2006**, 45, 7568.
- [88] Y. Xia, P. Yang, Y. Sun, Y. Wu, B. Mayers, B. Gates, Y. Yin, F. Kim, H. Yan, *Adv. Mater.* **2003**, 15, 353.
- [89] H. J. Fan, P. Werner, M. Zacharias, *Small* **2006**, 2, 700.
- [90] a) H. J. Fan, W. Lee, R. Scholz, A. Dadgar, A. Krost, K. Nielsch, M. Zacharias, *Nanotechnology* **2005**, 6, 913; b) H. J. Fan, B. Fuhrmann, H. Leipner, R. Scholz, A. Berger, A. Dadgar, A. Krost, U. Gösele, M. Zacharias, *Nanotechnology* **2006**, 16, S231.
- [91] R. Fan, Y. Y. Wu, D. Y. Li, M. Yue, A. Majumdar, P. D. Yang, *J. Am. Chem. Soc.* **2003**, 125, 5254.
- [92] Y. Chen, X. Xue, T. Wang, *Nanotechnology* **2005**, 16, 1978.
- [93] a) H. J. Fan, M. Knez, R. Scholz, K. Nielsch, E. Pippel, D. Hesse, U. Gösele, M. Zacharias, *Nanotechnology* **2006**, 17, 5157; b) M. Zacharias, K. Nielsch, private communication.

Received: May 30, 2007